Proceedings of the 9ICEG
9th International Congress on Environmental Geotechnics
25-28 June, 2023 | Chania, Greece
© Authors: All rights reserved, 2023
https://doi.org/10.53243/ICEG2023-53

Actual-Scale Field Trial of Rapid Soil Classification with Computer Vision, complemented with Electrical Resistivity and Soil Strength

Y. J. E. Aw[1], S. H. Chew[1], Y. C. Tan[2], C. S. Teo[2], M. L. Leong[2], H. B. G. Foo[2]

[1]*National University of Singapore, Singapore, email: ceeayje@nus.edu.sg*

[2]*Housing & Development Board, Singapore*

ABSTRACT

In Singapore, excess excavated soil from construction projects is re-purposed as material for infilling activities. Excavated soil is delivered to Staging Grounds (SGs) via tipper trucks, where they are categorized into either “Good Earth” or “Soft Clay”. Currently, soil classification is performed based on laboratory testing prior to excavation, and manual visual inspection of each truck upon arrival, which is highly human intensive. Heterogeneity of natural soils and possible mixing during excavation or loading process may also lead to a truck with differing soil types. This paper presents the prototype implementation of an innovative rapid soil classification system consisting of a computer vision technique with machine learning and complemented by geotechnical soil properties. The computer vision technique comprises soil image acquisition using an industrial-grade camera and decision-making with a trained Convolutional Neural Network (CNN) model. Three soil parameter determination at greater depth was used to complement computer vision: (i) apparent electrical resistivity using four electrodes arranged in Wenner’s array, (iii) moisture content using a time-domain reflectometer (TDR), and (iii) cone resistance using a modified cone penetrometer. A field trial was conducted using the on-site prototype setup on 493 soil samples and validated against the Particle Size Distribution (PSD) obtained from conventional laboratory testing. Results have shown that a high prediction accuracy of 85% was achieved. This non-destructive and instantaneous classification technique can be further expanded to other applications for sustainability in the construction industry.

Keywords: computer vision technique, cone penetration test, electrical resistivity, rapid and non-destructive, soil classification, convolutional neural network

1 INTRODUCTION

Excess excavated soil from construction projects is delivered to Staging Grounds to be re-purposed as infill material. At these staging grounds, this soil material is transported from construction sites in tipper trucks to the weighbridges, where the soil type is identified and weighed. As hundreds of tipper trucks arrive at the staging grounds on a daily basis, it is important to develop a solution to identify the soil type in a quick and accurate manner.

Excavated soils that are received at the staging grounds are classified into two broad soil types, “Good Earth” and “Soft Clay”, as Singapore has varying types of geological formations across the island. The classification relies on the Particle Size Distribution (PSD) and water content of the soil samples from the borehole logs, as well as visual inspection performed by the weighbridge operator. According to the classification criteria used by the staging grounds, Good Earth soils are made up of 65% of coarse particles (> 63μm) by weight and contains lower water content (< 40%). On the contrary, Soft Clay soils are made up of more fine particles and higher water content. As Soft Clay typically experiences a slower gain in shear strength and larger settlement as time passes, more expensive ground improvement techniques need to be used to consolidate it.

This study will provide insight into how this innovative technique of soil classification on-site using computer vision and soil parameter determination can accurately classify the excavated soils to ensure optimum soil recovery.

2 LITERATURE REVIEW

This section contains the literature review on the techniques used by the prototype to classify the soil.

2.1 Computer vision

Computer vision can be referred to as a type of computer science in imaging whereby image content can be interpreted utilizing pixel values (LeCun, Bengio, & Hinton, 2015). Computer vision usually requires a process that involves the following steps: (i) acquire, (ii) process, (iii) analyse and (iv) make sense of the data captured (Jähne, Haussecker, & Geissler, 1999). This systematic process can translate the pixels on an image into an interpretable output that can help us in making decisions and classifications in different research areas.

Image acquisition is performed via utilizing an image capturing device (e.g., camera) to transform electronic signals from a sensor into a numerical representation (Zareiforoush, Minaei, Alizadeh, & Banakar, 2015). After acquiring two-dimensional (2D) images, they are subsequently processed before feature extraction is performed. These representative features extracted are then fed into a decision-making module for classification problems.

2.2 Convolutional neural network (CNN)

To perform objective classification, a neural network is employed as part of the computer vision system to help predict the soil type. A convolutional neural network (CNN) can be defined as a feed-forward, deep artificial neural network (ANN), introducing convolution operations in at least one of the hidden layers (Bengio, Goodfellow, & Courville, 2015) as shown in Figure 1. The motivation behind CNN was visual perception – CNN kernels act as receptors that can perceive different features, while activation functions act as a role that emit electric signals once they exceed a certain threshold. CNN differs from the classical ANN in a few ways. Firstly, each neuron is only connected to a certain group of neurons from the previous layer, which reduces parameters required for processing. Secondly, groups of connections can share the same weight for the same purpose. Thirdly, pooling layers are introduced to reduce the amount of data processed while preserving useful information at the same time. These features have made CNN very popular in the recent times, especially for cases such as image classification (Li, Yang, Peng, & Liu, 2021).

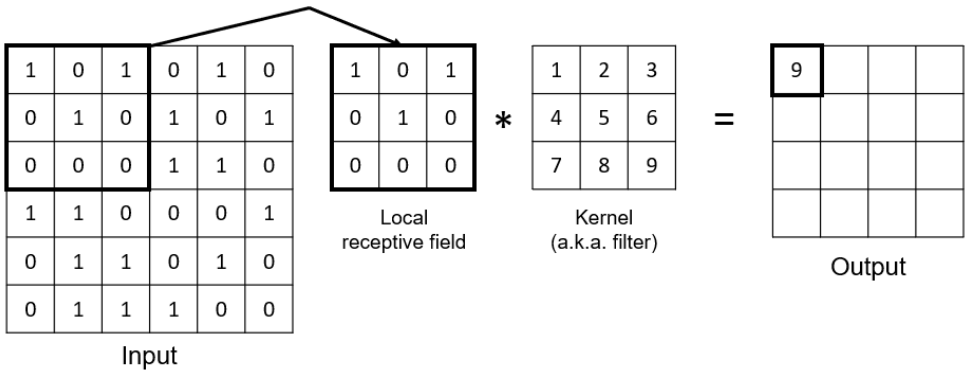

Figure 1. *An example of a convolution operation.*

The AlexNet was proposed by Alex et al. (2012), winning the championship during the ImageNet 2012 competition. The AlexNet (Figure 2) consists of five convolutional layers and three fully connected layers. It also fully utilizes rectified linear unit (ReLU) as its activation function, dropout layers to avoid overfitting, max pooling to replace average pooling for richer features, and local response normalization (LRN) to improve its ability to generalize.

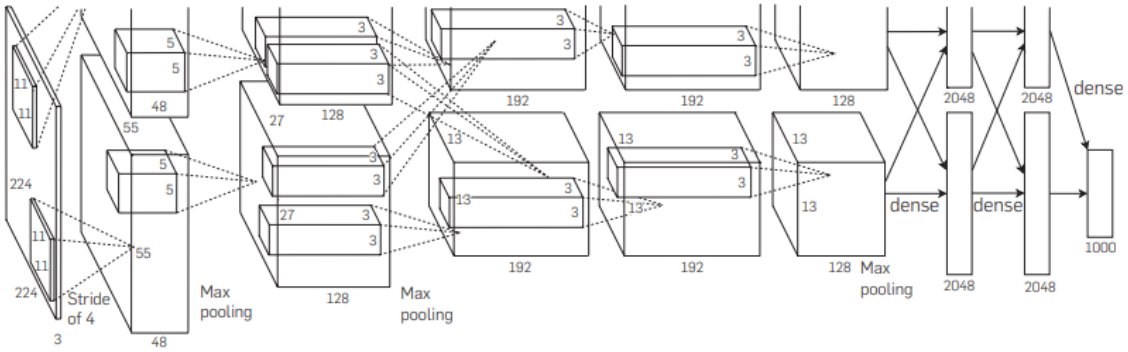

Figure 2. *The AlexNet architecture, adapted from* (Krizhevsky, Sutskever, & Hinton, 2012)*.*

2.3 Soil testing methods

2.3.1 Apparent resistivity

By Ohm' Law, the apparent resistivity of soil ρ (in a two-electrode soil box method) can be calculated using the following (1):

$$\rho = \frac{V}{I}\frac{A}{L} \tag{1}$$

where V = potential difference between two electrodes, I = current, L and A are the length and area of the conducting cross section of soil respectively. Wet to moist sand has a typical apparent resistivity of 20-200 Ωm, while that of clay ranges from 1-20 Ωm (Department of Army, U.S. Army Corps of Engineers, 2015).

2.3.2 Moisture content

The time-domain reflectometer (TDR) is an instrument that is capable of measuring in-situ moisture content, providing results almost instantaneously. By sending out a fast-rise voltage pulse through the waveguides, the wave propagation distance and speed measured are used to calculate the velocity of propagation, which is used to derive the apparent dielectric constant. This apparent dielectric constant is then used to estimate the volumetric moisture content drawn from a relationship supported by calibration data from numerous sources. A linear relationship was established, as shown in (2) (Knappett & Craig, 2020), to relate volumetric moisture content, θ_v, and apparent dielectric constant, ε_{ra}:

$$\theta_v = 0.115\sqrt{\varepsilon_{ra}} - 0.176 \tag{2}$$

2.3.3 Cone resistance

Cone penetration testing (CPT) is a common soil profiling technique that is quick and convenient. CPT is performed by inserting a cone into the soil sample. CPT tip resistance q_t is generally approximated by the cone tip resistance q_c at shallow soil depth (Topp & Ferré, 2005) where pore water pressure is ignored, which is applicable in the context of this application where the expected measuring depth is less than 1.5m.

2.4 Past research

In the earlier iterations of this rapid soil classification method, an artificial neural network (ANN) model was developed, using back-propagation network tested with 40 soil samples that were collected from the same staging ground (TMSG). The trained ANN model was found to be able to discern between Good Earth and Soft Clay soils in less than a minute.

Nonetheless, this updated computer vision system only captures data from the top surface of the soil in the truck but does not account for the possibility of different layers within the soil being delivered. Therefore, past research was conducted on suggested soil parameters that could be measured on-site to complement the computer vision system to account for this. Three soil parameter determination (apparent resistivity, moisture content, cone resistances) were conducted on a pre-made soil sample

(measuring 1800mm x 1200mm x 1000mm soil layer height) which was fabricated to simulate the soil mass in the truck hopper. Soil samples of two differing soil layers (either Good Earth or Soft Clay) were used for the tests conducted previously (i.e., GE-SC refers to Good Earth soil in the top half with Soft Clay in the bottom half, vice versa). Results in Figures 3 and 4 have shown that different soil layers could be identified using the three soil parameter determination on-site (Aw, et al., 2022).

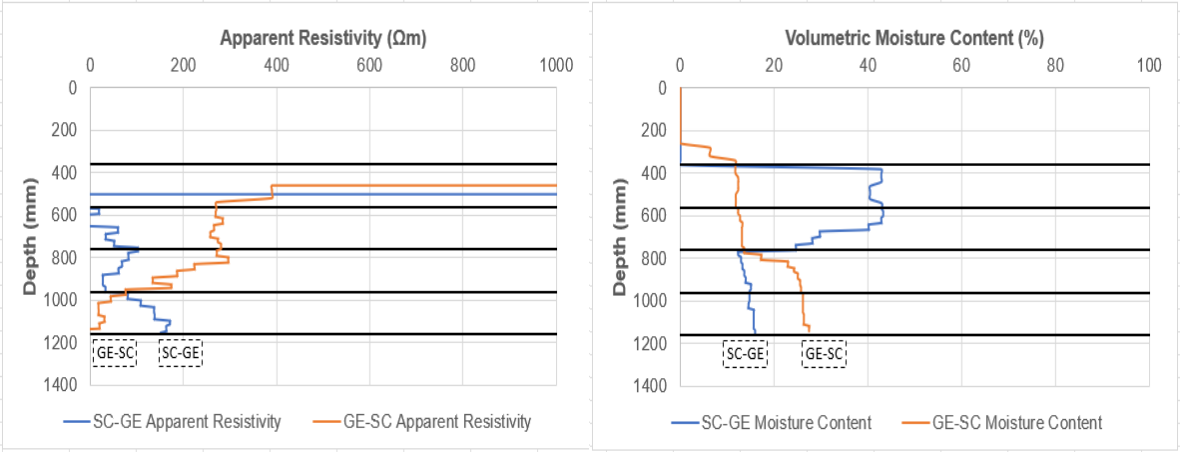

Figure 3. *(left) Apparent Resistivity with depth for GE-SC and SC-GE, (right) Volumetric Moisture Content with depth for GE-SC and SC-GE.*

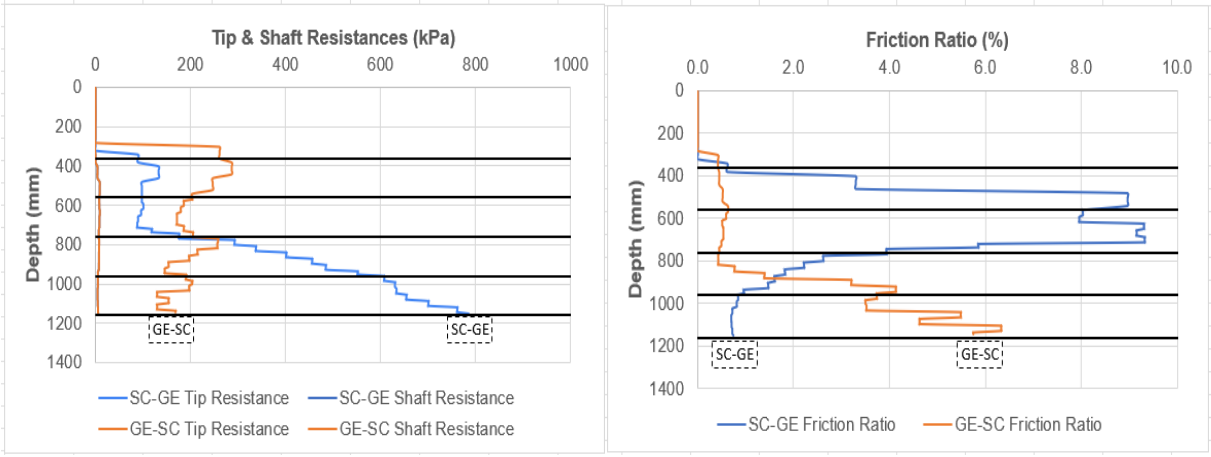

Figure 4. *(left) Tip & Shaft Resistances with depth for GE-SC and SC-GE, (right) Friction Ratio with depth for GE-SC and SC-GE.*

3 METHODOLOGY

As there was no computer vision system for soil classification available commercially in the market, a proprietary system (both software and hardware) was designed and used for this study. The hardware consists of an industrial-grade single-lens camera, together with an array of light emitting diode (LED) lighting positioned above the soil of the truck, as well as a set of sensors that can be actuated into the soil of the truck. The set of sensors include (notwithstanding): (i) an in-house customized cone penetrometer to measure tip and shaft resistances, (ii) a set for four conductive probes arranged in Wenner's array to measure apparent electrical soil resistivity, and (iii) a time-domain reflectometer (TDR) to measure volumetric moisture content. The software of the system consists of an in-house artificial intelligence software called NUS aiSS (Artificial Intelligence Scanning for Soil), which was developed to automate the computer vision system processes.

In total, 493 samples were collected using the prototype installed on-site. In each sample, a top-down image of the soil was captured and a set of soil parameter determination (tip and shaft resistances, apparent resistivity, moisture content) was measured.

3.1 Convolutional neural network (CNN) prediction model

The preparation of the convolutional neural network (CNN) prediction model was performed through following steps: (i) filtering out poor-quality images, (ii) allocation of dataset, (iii) data optimization, and (iv) development of the CNN prediction model architecture. Parameters of the network are shown in Table 1 below.

Table 1. *Hyperparameters of the CNN prediction model*

Hyperparameters	
Number of layers	7
Intermediate activation function	Rectified linear unit (ReLU)
Output activation function	Sigmoid
Epoch	300
Batch size	16
Number of k-folds	10

Images were resized to 800 x 800 while preserving aspect ratio. Images were also filtered by their mean grayscale level i.e., images that possess a mean grayscale level that is too low (≤ 10) or too high (≥ 185) were rejected for this study (Figure 5). This was to ensure the quality of the images. t.

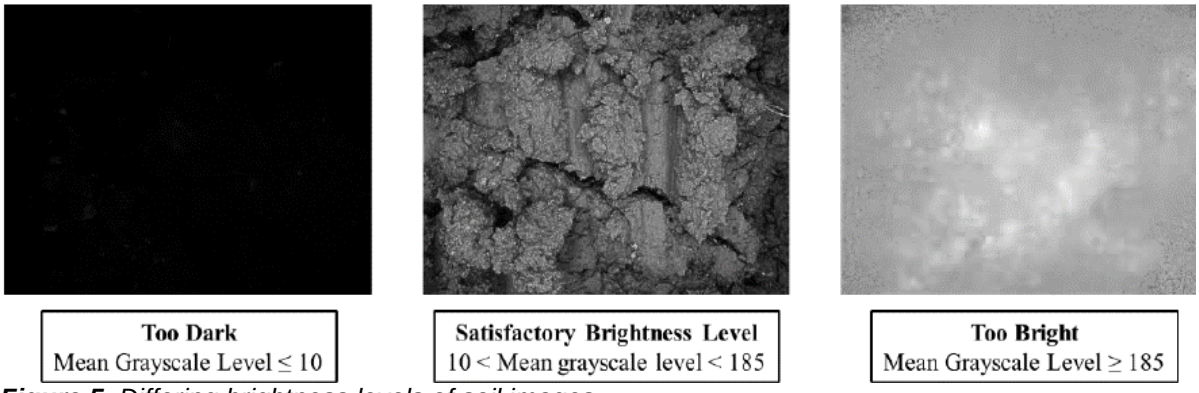

Figure 5. *Differing brightness levels of soil images.*

After filtering of the images, the remaining 466 images were allocated to three sets: (i) training set (54%), (ii) validation set (36%) and (iii) testing set (10%). As the dataset size may induce overfitting, a few techniques were used to combat the problem. Data augmentation refers to the manipulation of images to created augmented counterparts with translations (flipped vertically, horizontally, or both, rotated at different angles). By doing so, the model can also be trained to be spatially invariant and reduce the risks of overfitting.

The second technique to optimize the network was the use of dropout layers. A sample of neurons were randomly selected to be deactivated to create various sub-networks during training. These sub-networks were then merged to produce the final prediction of the entire neural network (Figure 6).

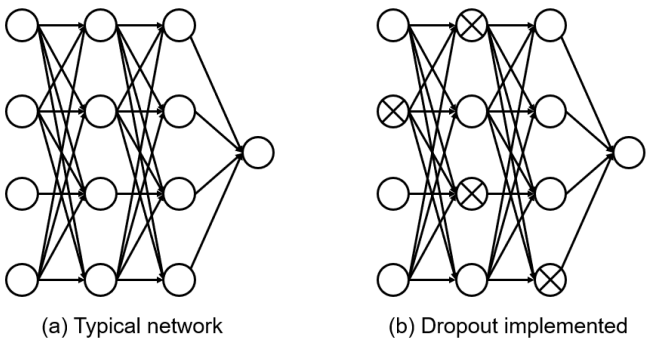

Figure 6. *Typical network (left). Network with dropout layers implemented (right).*

A L1 (level one) penalty-based regularization was also imposed; certain features had received a soft penalty whereby their weights were multiplied by a decay factor to reduce its contribution to the network. Together, these techniques helped to ensure that the network trained was more robust in classifying unseen soil samples. The resulting overall architecture is found in Figure 7 below, taking reference from AlexNet.

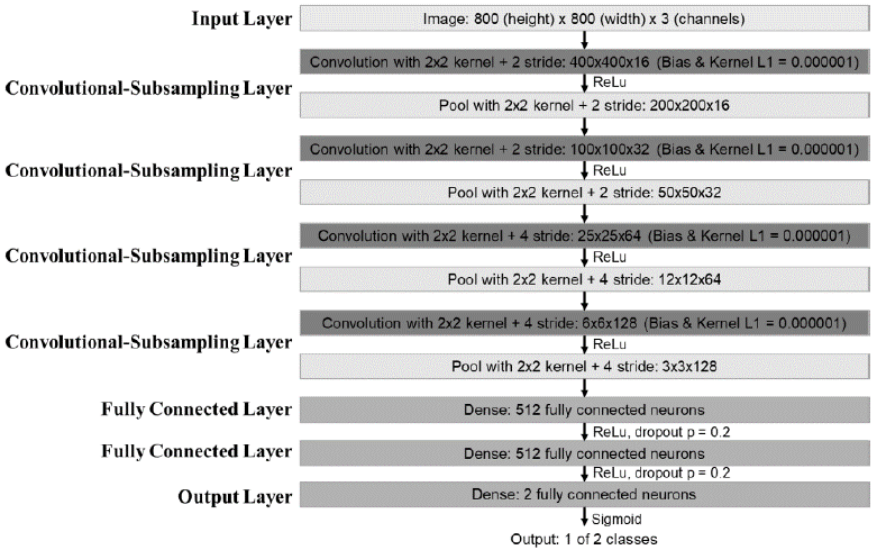

Figure 7. *Architecture of the CNN model developed with reference to AlexNet.*

3.2 Soil parameter determination

3.2.1 Measurement of apparent resistivity using Wenner's array

Four electrodes were arranged with equal spacing between them. Current is passed through the two outer electrodes (A and B) while the potential difference is taken between the two inner electrodes (C and D) (Figure 8). In this study, apparent resistivity refers to the apparent electrical resistivity of the soil sample measured. The apparent resistivity is calculated using the following (3):

$$\rho = \frac{4\pi aR}{1+\frac{2a}{\sqrt{a^2+4b^2}}-\frac{2a}{\sqrt{4a^2+4b^2}}} \quad (3)$$

where ρ = apparent resistivity (Ωm), a = electrode spacing (m), b = depth of electrode (m) and R = resistance (Ω), which is given by potential difference (ΔV) divided by current (I).

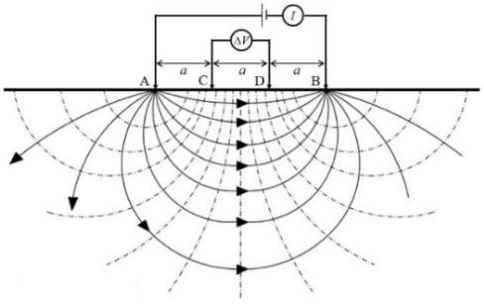

Figure 8. *A schematic of the Wenner's array.*

3.2.2 Measurement of moisture content using time-domain reflectometer (TDR)

A time-domain reflectometer (TDR) was chosen due to its instantaneous nature which is highly suitable for site implementation where processing time is a factor. The TDR is actuated into the soil sample together with the other sensors. As the volumetric moisture content measured is the average value

across the entire wave-guide length, the value is taken to be at the mid-point of the waveguides. A commercial datalogging software was utilized to measure and store the volumetric moisture content.

3.2.3 Measurement of tip and shaft resistances using in-house cone penetrometer

The cone penetration test (CPT) was performed using an in-house custom-built cone penetrometer where each data point is captured every second. The cone is 40mm in diameter with a 60° tip and a shaft of 40 mm diameter and 120 mm length. Both tip and shaft resistances were measured using the calibrated strain gauges installed within. The penetration rate of the CPT cone during measurement was 8 mm/s, which was much lower than the standard rate of 20±5 mm/s used in field CPT test to ensure better sensitivity in a soil sample with shallow thickness in this case.

3.3 Decision Table

Three soil parameter determination were used to complement the CNN prediction model in the form of a decision table. An example is found in Figure 9 where the soil image and particle size distribution are shown. By dividing the soil sample in the truck into four layers of 200mm soil thickness each (Figure 10), an overall soil type conclusion was made after considering the sub-conclusions from the four sub-layers. In Figure 10, q_c, ρ and w refers to the tip resistance, apparent resistivity and moisture content respectively. Threshold values of the three soil parameter determination for Good Earth ("GE") and Soft Clay ("SC") were found from past research, while "GRAY" denotes values that were outside of the threshold values. The soil sample was eventually determined as a Soft Clay soil.

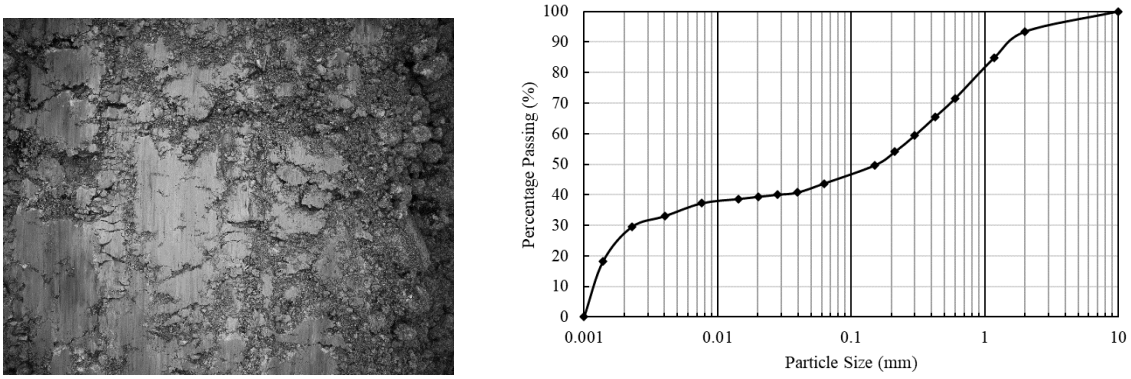

Figure 9. *Image of the soil sample (left). Particle size distribution (right).*

	CNN	q_c (kPa)	ρ (Ωm)	w (%)	Layer Soil Type
Layer 1	GE GE:0.71, SC:0.29	SC 90.00	GRAY 122.57	GE 8.84	GE
Layer 2	- -	GRAY 145.00	SC 33.80	SC 33.64	SC
Layer 3	- -	SC 156.50	SC 41.53	SC 43.85	SC
Layer 4	- -	SC 131.33	SC 58.02	SC 43.58	SC
Final Soil Type	SOFT CLAY (some GE top)				

Figure 10. *Image of the decision table results from the in-house software.*

4 RESULTS & DISCUSSION

4.1 Initial results from computer vision only

The soil classification technique is a two-step method (first step using the convolutional neural network (CNN) prediction model, and the second step using the decision table). Prediction accuracy results from the CNN prediction model (i.e., computer vision only) conducted on the 47 samples in the testing set are tabulated in Table 2. In this result, prediction accuracy refers to the percentage of soil samples that was predicted correctly in each k-fold. As the cross-validation k value is 10, results from the 10 k-folds are shown in Table 2 below. The average prediction accuracy is 81.70%, and it can be seen that the

prediction accuracies fall within a ±4% band across the 10 k-folds. However, the results below are only based on the images alone without the three complementary soil parameter determination.

Table 2. *Prediction accuracies from the 10 k-folds*

K-fold	Prediction accuracy (%)
Fold 1	81.48
Fold 2	84.07
Fold 3	78.78
Fold 4	80.78
Fold 5	84.19
Fold 6	78.37
Fold 7	82.96
Fold 8	82.07
Fold 9	81.37
Fold 10	82.91

4.2 Overall results from computer vision with decision table

The decision table (built using sensor data from soil parameter determination) was introduced to the computer vision to enable the system to capture information below the soil surface, hence producing a more robust prediction. The actual soil type to which the prediction result was compared against (i.e., the control) was determined through conventional laboratory testing of the sample using particle size distribution and moisture content, while the predicted soil type is determined by the output of the CNN prediction model. The results are tabulated in the confusion matrix as shown in Figure 11.

The prediction accuracy was 85.11% with a precision value of 0.92 and a recall value of 0.82. Prediction accuracy was improved as the system can now consider soil sub-layers within the soil sample and give a more robust prediction of the soil type.

		Predicted Soil Type	
		GE	SC
Actual Soil Type	GE	17	2
	SC	5	23

Figure 11. *Results in a confusion matrix.*

5 CONCLUSIONS

This paper has presented findings on the use of a computer vision system with a trained convolutional neural network (CNN) prediction model aided by three complementary soil parameter determination (apparent resistivity, moisture content, cone resistances) for rapid soil classification into either Good Earth or Soft Clay on-site. The results have shown that not only does the CNN prediction model is viable for such a use case, but also that complementary geotechnical measurements are important for the entire system to stay robust and make more comprehensive decisions. However, therein lies room for improvement with a larger database of images and stronger prediction models that can increase the prediction accuracy, as well as hardware improvements that allows the data to be captured more accurately.

Currently, this system is used for classifying excavated soil into two broad soil types displaying its viability in field conditions (as opposed to the controlled laboratory environment). The technique can further be applied to other geotechnical classification cases as long as the prediction model is sufficiently trained, and careful implementation is performed. Techniques such as this rapid soil classification method can spur more data-driven applications and also attract more talents, both from and outside

geotechnical engineering, to improve to the productivity and sustainability of the construction industry in Singapore.

6 ACKNOWLEDGEMENTS

This research is supported by the Singapore Ministry of National Development and the National Research Foundation, Prime Minister's Office under the Cities of Tomorrow (COT) Research Programme (COT Award No. COT-V3-2019-1). Any opinions, findings and conclusions or recommendations expressed in this paper are those of the author(s) and do not reflect the views of the Singapore Ministry of National Development and National Research Foundation, Prime Minister's Office, Singapore.

REFERENCES

Aw, Y., Chew, S., Chua, K., Goh, P., Cheng, L., & Tan, S. (2022). Field Trial on Rapid Soil Classification Using Computer Vision. Geo-Congress 2022. Charlotte, North Carolina, USA.

Aw, Y., Chew, S., Tan, Y., Goh, P., Teo, C., Tan, S., & Leong, M. (2022). Field Trial to Rapidly Classify Soil Using Computer Vision with Electric Resistivity and Soil Strength. Fifth Intl. Conf. on New Developments in Soil Mechanics and Geotechnical Engineering. Nicosia, North Cyprus.

Bengio, Y., Goodfellow, I., & Courville, A. (2015). Deep Learning. Cambridge, MA, USA: MIT Press.

Department of Army, U.S. Army Corps of Engineers. (2015). Geophysical Exploration for Engineering and Environmental Investigations. Scholar's Choice.

Jähne, B., Haussecker, H., & Geissler, P. (. (1999). Preface. In Handbook of computer vision and applications (Vol. 2) (pp. 423-450). New York: Academic press.

Knappett, J., & Craig, R. (2020). CRAIG'S SOIL MECHANICS. CRC Press.

Krizhevsky, A., Sutskever, I., & Hinton, G. E. (2012). ImageNet Classification with Deep Convolutional Neural Networks. Advances in neural information processing systems 25(2).

LeCun, Y., Bengio, Y., & Hinton, G. (2015). Deep learning. Nature 521, 436-444.

Li, Z., Yang, W., Peng, S., & Liu, F. (2021). A Survey of Convolutional Neural Networks: Analysis, Applications, and Prospects. IEEE transactions on neural networks and learning systems.

Topp, G., & Ferré, T. (2005). TIME-DOMAIN REFLECTOMETRY. In Encyclopedia of Soils in the Environment (pp. 174-181). Elsevier.

Zareiforoush, H., Minaei, S., Alizadeh, M. R., & Banakar, A. (2015). Potential applications of computer vision in quality inspection of rice: a review. Food engineering reviews, 7(3), 321-345.